https://doi.org/10.5194/egusphere-2025-3886
Preprint. Discussion started: 9 September 2025

Drivers and Variability of Marine Heatwaves in the North Indian Ocean and their Impacts on South Asian Monsoon Rainfall

Ligin Joseph[1], Nikolaos Skliris[1], Vishnu S[2], Dipanjan Dey[3,1], and Robert Marsh[1]

[1]School of Ocean and Earth Science, University of Southampton, Southampton, UK
[2]School of Earth Environmental and Sustainability Sciences, Indian Institute of Science Education and Research, Thiruvananthapuram, India
[3]School of Earth, Ocean and Climate Sciences, Indian Institute of Technology Bhubaneswar, Argul, Khordha, India

Correspondence: Ligin Joseph (l.joseph@soton.ac.uk)

Abstract. Our planet is warming rapidly, and, with it, the frequency and intensity of marine heatwaves (MHWs) are increasing. While MHWs disrupt marine ecosystems, they also significantly influence regional climate systems, including the Asian monsoon. This study investigates the variability, drivers, and monsoon impacts of MHWs in the North Indian Ocean using detrended sea surface temperature anomalies from 1982 to 2024. An Empirical Orthogonal Function (EOF) analysis of MHW intensity reveals two leading modes. The first mode (PC1), explaining 22% of the variance, shows widespread MHWs with stronger intensity in the Arabian Sea. It is associated with anomalously high pressure over the North Indian Ocean and low pressure in the Southern Hemisphere, which weakens monsoon winds, reduces evaporation and cloud cover, and increases shortwave radiation, thereby warming the upper ocean. The second mode (PC2), explaining 8% of the variance, displays a dipole pattern, with MHWs in the Bay of Bengal and suppressed activity in the Arabian Sea during its positive phase, and the reverse during its negative phase. Large-scale climate modes modulate MHW development. El Niño combined with the transition phase of MISO (from break to active) triggers basin-wide MHWs (PC1), while La Niña during a similar MISO phase promotes PC2-like warming in the Bay of Bengal. These modes influence rainfall as well. PC1 and PC2+ are linked to wetter conditions in southern India and drier conditions in the north, while PC2- corresponds to widespread dryness. MHW termination can enhance rainfall through the revival of monsoon winds and heat release. These findings suggest potential feedback between MHWs and MISO, with implications for improved monsoon prediction under climate change.

1 Introduction

Our planet is warming at an unprecedented rate, and 2024 was recorded as the hottest year on record for both land and ocean temperatures (Rohde, 2025; World Meteorological Organization, 2025). The rise in ocean temperature has gained increasing scientific attention due to its far-reaching implications for the climate system and the intensification of extreme weather events (Johnson et al., 2023). Among the world's oceans, the Indian Ocean is warming the fastest, making it a critical region for understanding ocean-atmosphere interactions in a warming world (Roxy et al., 2014; Venegas et al., 2023).

The Indian Ocean is the principal source of moisture for the South Asian Monsoon, which is the largest monsoon system, on which millions of people depend for agriculture, water security, and livelihoods (Dey and Döös, 2021). Any change in

https://doi.org/10.5194/egusphere-2025-3886
Preprint. Discussion started: 9 September 2025

the Indian Ocean's thermal structure, therefore, has the potential to substantially influence monsoon variability and intensity (Roxy et al., 2015; Yadav and Roxy, 2019; Skliris et al., 2022; Joseph et al., 2024). While previous studies have focused on the mean-state warming of the Indian Ocean, particularly the western basin including the Arabian Sea (Oppo and Rosenthal, 2010; Swapna et al., 2013; Roxy et al., 2014; D'Mello and Kumar, 2018; Pratik et al., 2018; Zhang et al., 2018; Mathew et al., 2018; McMonigal et al., 2022; Albert et al., 2023; Nisha et al., 2023; Shee et al., 2023; Chatterjee et al., 2024; Joseph et al., 2025), relatively limited attention has been paid to understanding periods of anomalously high Sea Surface Temperature (SST) lasting days to weeks, known as marine heatwaves (MHWs).

Recent studies suggest that MHWs are becoming more frequent, more intense, and longer in duration across various regions of the global ocean, driven by anthropogenic warming and internal climate variability (Oliver et al., 2018; Saranya et al., 2022; Chatterjee et al., 2022; Chakraborty et al., 2023; Cheng et al., 2023; Koul et al., 2023; Capotondi et al., 2024; Gupta et al., 2024). Saranya et al. (2022) demonstrated that the frequency of MHWs in the western Indian Ocean and northern Bay of Bengal is increasing, often in association with background ocean warming and El Niño events. These MHWs, in turn, influence ISM rainfall patterns by suppressing rainfall over central India and enhancing it over the south, depending on the location of the MHW. Similarly, Chatterjee et al. (2022) found an increasing trend in MHW events over the northern Arabian Sea linked to increasing mean SST and El Niño forcing. Chakraborty et al. (2023) showed that MHW intensity is higher in the western Arabian Sea than in the east and that these events significantly influence biogeochemical cycles. Liang et al. (2024) found high correlations between the Indian Ocean Dipole (IOD) and MHW days in the Bay of Bengal. Kumar et al. (2023) documented that the MHWs in the Bay of Bengal are driven by changes in the net heat flux and anticyclonic eddies. Furthermore, Gupta et al. (2023) showed that the surface MHWs in the Bay of Bengal are frequent during El Niño and positive IOD years, whereas subsurface MHWs are usually driven by the thermocline changes driven by La Niña and negative IOD.

Collectively, these studies affirm that MHWs in the North Indian Ocean are intensifying, although they differ in regional focus and metrics. Importantly, all these studies use a fixed baseline seasonal climatology to define MHWs, which can mix long-term ocean warming with short-term events. This makes MHWs appear more frequent in recent decades and could even lead to scenarios where oceans enter a "permanent MHW state", particularly in rapidly warming regions like the Indian Ocean. Indeed, recent projections suggest the Indian Ocean could permanently exceed MHW thresholds by 2050 under fixed-baseline definitions (Roxy et al., 2024). To address this, several studies have proposed defining MHWs using detrended SST anomalies or a moving baseline, which helps distinguish true marine heatwave events from long-term warming (Jacox, 2019; Rosselló et al., 2023; Amaya et al., 2023; Capotondi et al., 2024). A recent study suggests reserving the term "Marine Heatwaves" for events identified using a moving baseline approach, while using "long-term temperature trend" for slow changes in the ocean temperature and using "total heat exposure" to describe the combination of long-term warming and marine heatwaves (Amaya et al., 2023). This avoids the misclassification of slowly increasing background SST as MHWs.

Despite the emergence of improved methodologies, the use of detrended or moving-baseline approaches in defining MHWs in the North Indian Ocean remains limited. Moreover, no comprehensive study has yet examined the variability, drivers, and monsoonal consequences of these events in this climate-sensitive basin. This study fills that critical gap. In this present study, we apply a detrended SST anomaly framework to identify MHWs in the North Indian Ocean, allowing us to disentangle

https://doi.org/10.5194/egusphere-2025-3886
Preprint. Discussion started: 9 September 2025

short-term marine heatwave dynamics from the long-term warming signal. Building on this improved detection, we conduct a detailed investigation into the dominant modes of MHW variability, diagnose their physical drivers, including oceanic and atmospheric forcing mechanisms, and investigate their possible impacts on the monsoon rainfall over South Asia. By bridging marine heat extremes and monsoonal variability, our study offers a new understanding of how upper-ocean thermal anomalies influence regional climate, with implications for prediction and climate risk assessment across South Asia.

2 Data and Methods

2.1 Data Used

To identify MHWs and investigate their drivers in the North Indian Ocean, we use daily SST and atmospheric variables including 10-meter winds, mean sea level pressure (MSLP), surface latent heat flux, net shortwave radiation at the surface, total cloud cover, and total precipitation from the ERA5 reanalysis dataset (Hersbach et al., 2020). The ERA5 SST is based on HadISST2 from 1979 to August 2007 and on OSTIA from September 2007 onward, benefiting from rigorous data assimilation (Titchner and Rayner, 2014; Good et al., 2020; Hersbach et al., 2020). We use ERA5 SST to identify MHW events and analyze their drivers to ensure consistency with the atmospheric fields, all of which are derived from ERA5. In addition, we compute the MHW characteristics (e.g., frequency, duration and intensity; see Figure 1) using NOAA OISST to take advantage of its widely used observational record (Reynolds et al., 2002). Our analysis covers the period 1982–2024, during which both ERA5 and OISST provide consistent and reliable data. Notably, similar results are found when using OISST, indicating that our conclusions are not sensitive to the choice of SST dataset (see Fig. S10, Fig. S11, and Fig. S12).

2.2 Marine Heat Waves Classification

The MHWs are typically defined as periods when daily SST anomalies exceed the seasonally varying 90th percentile threshold for five or more consecutive days (Hobday et al., 2016). This threshold is usually computed using a fixed baseline climatology. However, recent studies have highlighted a key limitation of this approach. As global SSTs rise, the frequency of MHWs defined relative to a fixed baseline can increase artificially, causing the "unusual" to become the "new normal" (Jacox, 2019; Rosselló et al., 2023; Amaya et al., 2023; Capotondi et al., 2024). To address this, it has been proposed that the definition of MHWs should depend on the intended impact being assessed. For instance, when studying biological impacts such as the adaptability of marine organisms, a fixed baseline may be appropriate, as it captures absolute thermal stress relative to a historical normal. In contrast, for assessing climate impacts, particularly those related to atmospheric feedbacks and precipitation, a moving baseline or detrended SST anomalies should be used to better isolate episodic extreme events from long-term warming. Some recent studies have further recommended reserving the term "marine heatwave" for events defined using a moving climatology (Amaya et al., 2023).

In this study, we define MHWs using detrended SST anomalies. An event is identified as an MHW when the detrended SST anomaly exceeds the seasonally varying 90th percentile for at least five consecutive days. The percentile threshold and

https://doi.org/10.5194/egusphere-2025-3886
Preprint. Discussion started: 9 September 2025

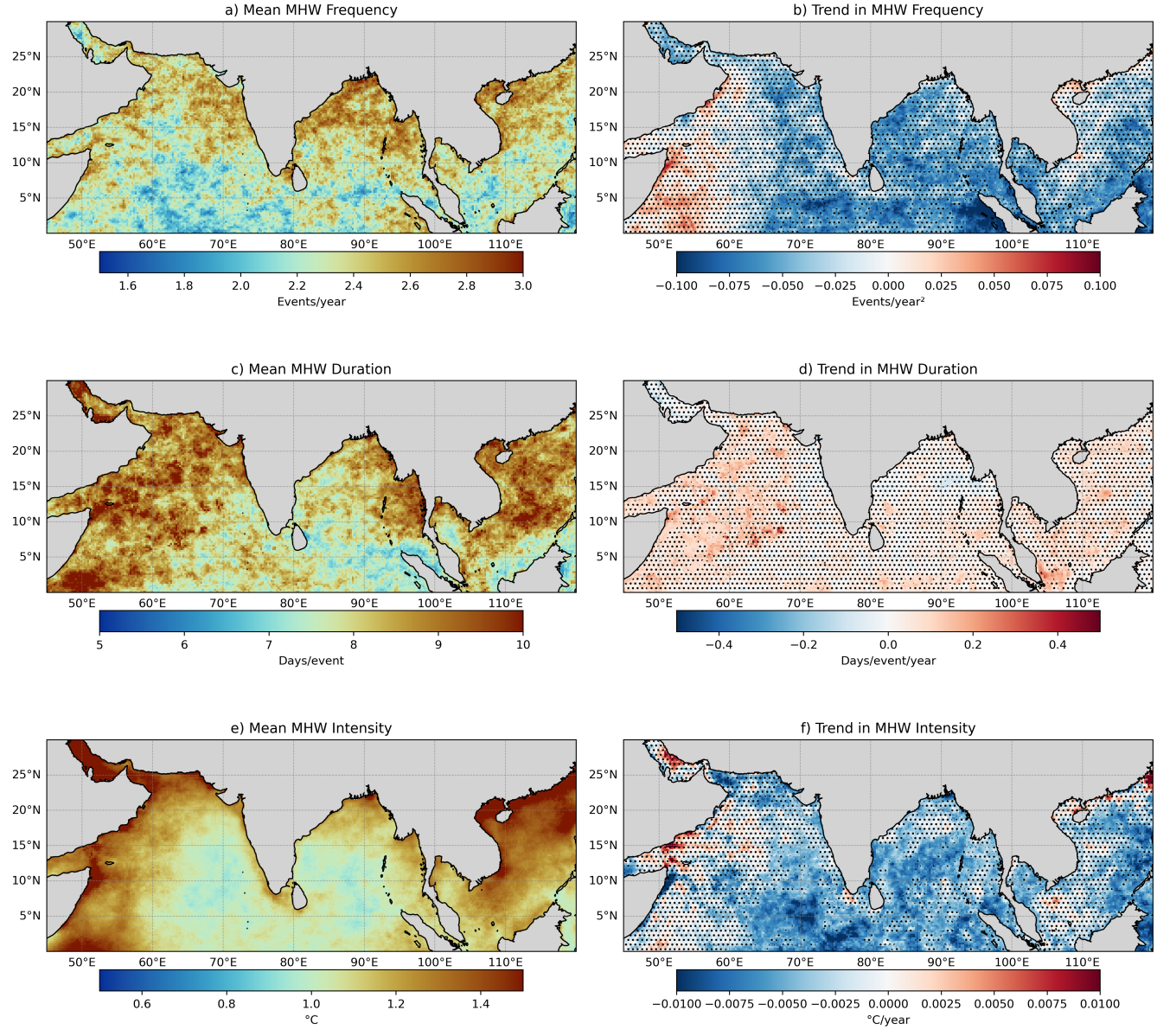

Figure 1. Spatial maps of (a) mean annual frequency of MHW events (events/year), (b) linear trend in MHW frequency (events/year^2), (c) mean duration of MHW events (days/event), (d) trend in MHW duration (days/event/year), (e) mean intensity of MHW events (°C), and (f) trend in MHW intensity (°C/year) over the period 1982-2024. Hatching indicates regions where trends are not statistically significant ($p > 0.05$) based on a two-tailed linear regression test.

the anomalies are calculated using the full 1982–2024 period. A seasonal climatology is first constructed using an 11-day centered moving window to capture day-to-day variability. This is then smoothed using a 31-day binomial filter to ensure

https://doi.org/10.5194/egusphere-2025-3886
Preprint. Discussion started: 9 September 2025

temporal coherence and reduce high-frequency noise (Hobday et al., 2016). The mean and linear trends of key MHW metrics, including the frequency, duration, and mean intensity, computed using the detrended SST anomalies, are shown in Figure 1. The frequency of MHW events is higher in the Bay of Bengal compared to the Arabian Sea, whereas the MHWs in the Arabian Sea tend to last longer and show higher mean intensity. Although we do not observe widespread statistically significant trends in these metrics based on detrended SSTs, unlike studies using a fixed baseline that report significant increases (Saranya et al., 2022; Chatterjee et al., 2022; Gao et al., 2022; Kumar et al., 2023), but some regional patterns emerge. In particular, MHW duration shows a significant increasing trend across some portion of the Arabian Sea, while the Bay of Bengal exhibits a significant decrease in MHW intensity.

To understand and quantify the importance of detrending SSTs in the identification of MHWs, we present the following example using OISST. We focus on basin-scale MHW events, defined as those covering at least 25% of the basin and lasting for a minimum of 15 consecutive days, in both the Arabian Sea and the Bay of Bengal. Using detrended SST anomalies, we identified 20 events in the Arabian Sea and 17 in the Bay of Bengal, compared to 17 and 24 events, respectively, using raw (non-detrended) SSTs. Notably, before 2010, 12 MHW events were detected in the Arabian Sea and 9 in the Bay of Bengal using detrended anomalies, whereas only 1 and 2 events, respectively, were identified using non-detrended SSTs. In contrast, after 2010, 8 events were identified in each basin using detrended data, while 16 events in the Arabian Sea and 22 in the Bay of Bengal were found using raw SSTs. This clearly illustrates that failing to remove long-term warming trends can lead to an overestimation of recent MHW frequency. For instance, in 2023 alone, 202 MHW days were identified in the Arabian Sea and 93 in the Bay of Bengal using raw SSTs, compared to only 55 and 0 days, respectively, using detrended anomalies. These results underscore the necessity of detrending to accurately characterize episodic heat extremes rather than long-term background warming.

2.3 Climate Indices

To assess the influence of large-scale modes of natural climate variability, such as the ENSO and the IOD, we utilize the Niño-3.4 index (for ENSO) and the Dipole Mode Index (DMI, for the IOD). The Niño-3.4 index is defined as the area-averaged SST anomalies over the Niño-3.4 region (5°N–5°S, 170°–120°W), relative to a 1981–2010 climatology. The DMI represents the anomalous SST gradient between the western equatorial Indian Ocean (50°–70°E, 10°S–10°N) and the southeastern equatorial Indian Ocean (90°–110°E, 10°S–0°). Both indices are obtained from the NOAA Physical Sciences Laboratory (NOAA PSL), where they are computed using the HadISST1.1 dataset (Rayner et al., 2003).

3 Variability of Marine Heatwaves in the North Indian Ocean

To understand the variability of MHWs in the North Indian Ocean, we performed an Empirical Orthogonal Function (EOF) analysis on daily MHW intensity (SST during MHW), derived from detrended SST anomalies during MHW events. Two dominant modes were identified, and their spatial patterns along with the corresponding normalized principal components (PC) are shown in Figure 2. The first mode, which explains approximately 22% of the total variance, exhibits a basin-wide

https://doi.org/10.5194/egusphere-2025-3886
Preprint. Discussion started: 9 September 2025

pattern characterized by high MHW intensity across the central and southwest Arabian Sea, highlighting this region as a hotspot of strong MHW events. The second mode displays a dipole-like structure between the Arabian Sea (except north) and the Bay of Bengal regions, showing suppressed MHW activity (blue shading) in one basin, coinciding with enhanced activity in the other, and vice versa. Unlike Mode 1, the normalized PC time series of Mode 2 displays a more symmetric distribution between positive and negative phases, suggesting alternating dominance of MHWs between the two basins. This mode explains approximately 8% of the total variance.

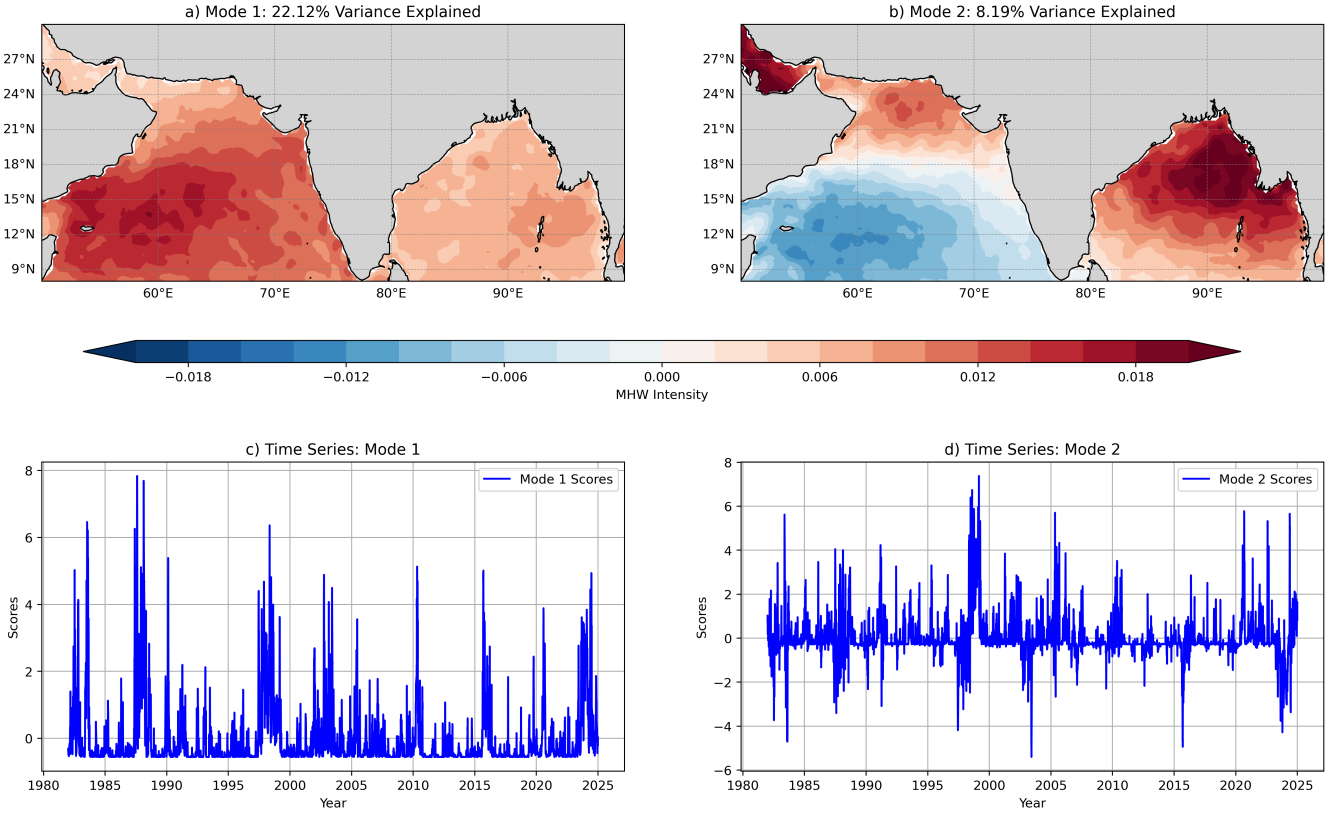

Figure 2. Empirical Orthogonal Function (EOF) analysis of the MHW intensity in the North Indian Ocean using ERA5 SST (based on daily data for all months, not limited to JJAS). (a) Spatial pattern of the leading mode (Mode 1). (b) Spatial pattern of the second mode (Mode 2). (c) Normalized principal component time series corresponding to Mode 1. (d) Normalized principal component time series corresponding to Mode 2.

Previous studies have shown that large-scale natural climate variability modes, such as the ENSO and the IOD, can strongly influence the frequency, intensity, and duration of MHWs (see Capotondi et al. (2024) for a recent review; Gao et al. (2022); Chatterjee et al. (2022); Swetha et al. (2025)). To explore these relationships, we computed monthly lead-lag correlations between the PCs of the two dominant modes and the Niño 3.4 index (representing ENSO) and the Dipole Mode Index (DMI, representing the IOD). The results are shown in Figure 3. The highest correlation (0.5) is observed between PC1 and Niño 3.4

https://doi.org/10.5194/egusphere-2025-3886
Preprint. Discussion started: 9 September 2025

when Niño 3.4 leads by approximately 5 months. This suggests that the basin-wide MHW pattern represented by PC1 may be linked to the mature phase of ENSO. This relationship is consistent with the Indian Ocean Basin Mode (IOBM), where ENSO induces basin-wide warming in the Indian Ocean with a few months lag (Klein et al., 1999; Xie et al., 2009; Guo et al., 2017). The strong lagged correlation between PC1 and Niño 3.4, along with the similarity to the IOBM, suggests that basin-wide MHWs in the North Indian Ocean can be largely modulated by ENSO via the Indian Ocean Basin Mode. This is consistent with Chatterjee et al. (2022) who showed that 70-80% of MHWs in the Arabian Sea are influenced by the Indian Ocean Basin mode through the decaying phase of ENSO. PC1 also shows a weaker but noticeable correlation with DMI (0.3) when DMI leads by about 2 months. However, since the correlation between Niño 3.4 and DMI also peaks at this lag, the PC1–DMI correlation may simply reflect the influence of ENSO on the IOD rather than an independent effect of the IOD itself (see Fig. S1 for lead–lag partial correlation between the DMI and the PC time series after statistically removing the influence of Niño3.4). In contrast, the PC2 correlation with Niño 3.4 or DMI is relatively less compared to PC1. The maximum correlation (0.3) occurs when PC2 leads Niño 3.4 by about 2 months, suggesting only a weak link. These findings imply that large-scale climate modes, particularly ENSO, might play a crucial role in driving the variability of MHWs in the North Indian Ocean, especially through their influence on the basin-wide pattern (PC1). The drivers of each mode will be examined in greater detail in the following sections.

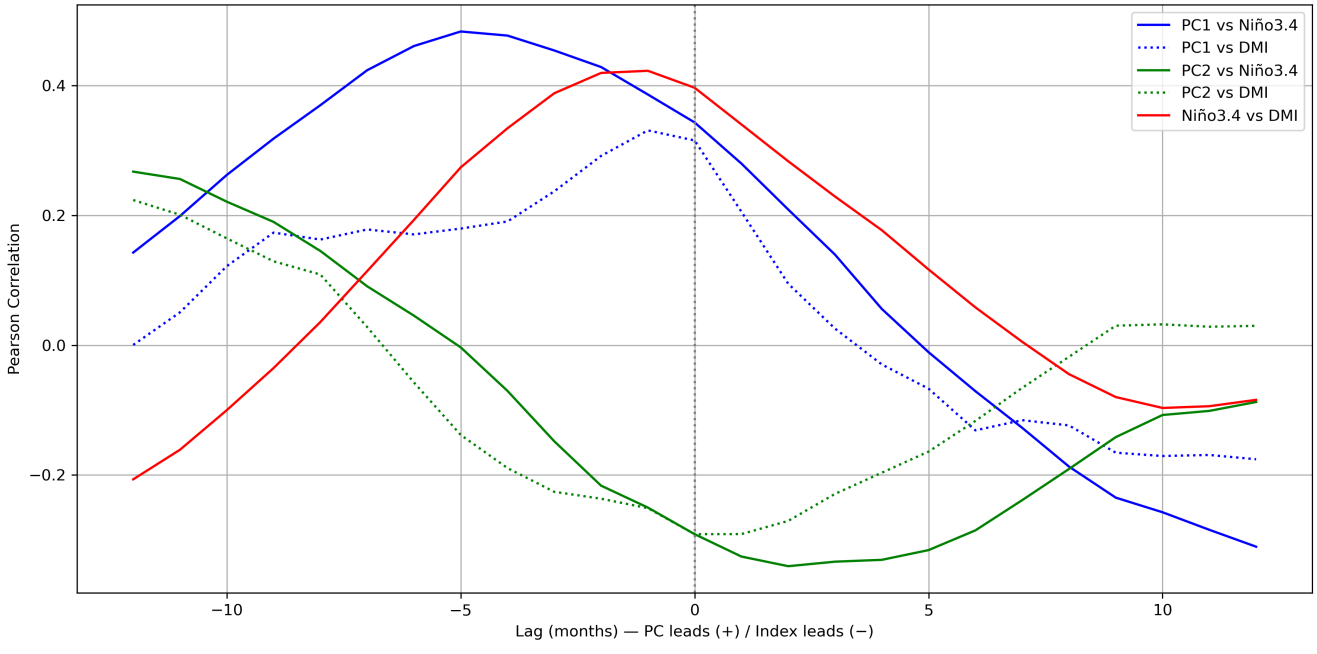

Figure 3. Lead-lag correlations between the PCs (converted to monthly) and climate indices. Blue and green lines represent correlations involving PC1 and PC2, respectively. Solid lines denote correlations with Niño 3.4, while dashed lines denote correlations with the DMI. The red line shows the correlation between Niño 3.4 and DMI. Negative lags indicate the climate index leads the PC, while positive lags indicate the PC leads the index.

https://doi.org/10.5194/egusphere-2025-3886
Preprint. Discussion started: 9 September 2025

4 The Drivers of Marine Heatwaves Modes in the North Indian Ocean

To analyze the drivers of the two dominant modes of MHW variability in the North Indian Ocean, we identified extreme events based on the daily normalized PC time series. Events were selected when the PCs exceeded the seasonally varying 90th (10th in case of the negative phase of Mode 2) percentile for at least five consecutive days, consistent with the definition of MHWs. Our analysis is restricted to events occurring during the South Asian Monsoon season (June–September), aligning with our objective of assessing their influence on South Asian monsoon rainfall.

The leading mode of MHWs (PC1) in the North Indian Ocean corresponds to a basin-wide pattern, with MHWs covering the entire region and particularly high intensity in the Arabian Sea (Figure 2a). We identified 16 distinct events in which the PC1 time series exceeded the seasonally varying 90th percentile for at least five consecutive days. The start dates, end dates, and durations of these events are provided in Table S1. These PC1-mode MHW events lasted between 5 and 59 days, with a median duration of 10 days and a mean duration of approximately 19 days. Interestingly, the latest three events show a duration above 20 days. Notably, 10 events out of 16 occurred during El Niño or within 5 months after El-Nino. Regression of the PC1 time series onto SST (Fig. S2a) reveals an El Niño–like SST pattern, further supporting the association between this MHW mode and El Niño conditions.

In contrast to the basin-wide structure of Mode 1, the positive phase of Mode 2 (PC2+) displays an east–west dipole, with MHWs focused in the Bay of Bengal and an absence of MHWs in the central and southern Arabian Sea (Figure 2b). We identify 34 PC2+ events (Table S2), most commonly during the El Niño to La Niña transition phase, with durations ranging from 5 to 35 days (mean of 12 days and median of 10 days). The negative phase of Mode 2 (PC2-) reverses the east–west dipole, with MHW activity concentrated in the central and southern Arabian Sea and absent in the Bay of Bengal. A total of 22 such events were identified based on the PC2 time series falling below the seasonally varying 10th percentile for at least five consecutive days (Table S3).

4.1 SST and Precipitation during the Marine Heatwaves

The composite anomalies of detrended SST and precipitation overlaid with 10-meter winds during the selected extreme events for different EOF modes are shown in Figure 4. As expected from the PC1 spatial pattern, SST anomalies are strongly positive across the North Indian Ocean, including the Arabian Sea and the Bay of Bengal. The strongest warming is observed in the Arabian Sea (Figure 4a). The corresponding precipitation and 10-meter wind anomalies indicate weakening of monsoon winds (anomalous Northerly winds or weakened Southerly winds) and enhanced rainfall over the eastern Arabian Sea, southern Bay of Bengal and parts of southern India, while central and northeastern India and north of the Bay of Bengal exhibit suppressed precipitation (Figure 4d). Although the SST anomalies somewhat resemble those typically observed during a positive IOD event, the associated wind patterns deviate from the canonical IOD structure, which is characterized by strengthened cross-equatorial monsoon winds (Prajeesh et al., 2021).

The composite SST anomalies during PC2+ events show intense warming over the Bay of Bengal and parts of the northern Arabian Sea, while southern Arabian Sea SSTs remain neutral or slightly negative (Figure 4b). This warming is accompanied

https://doi.org/10.5194/egusphere-2025-3886
Preprint. Discussion started: 9 September 2025

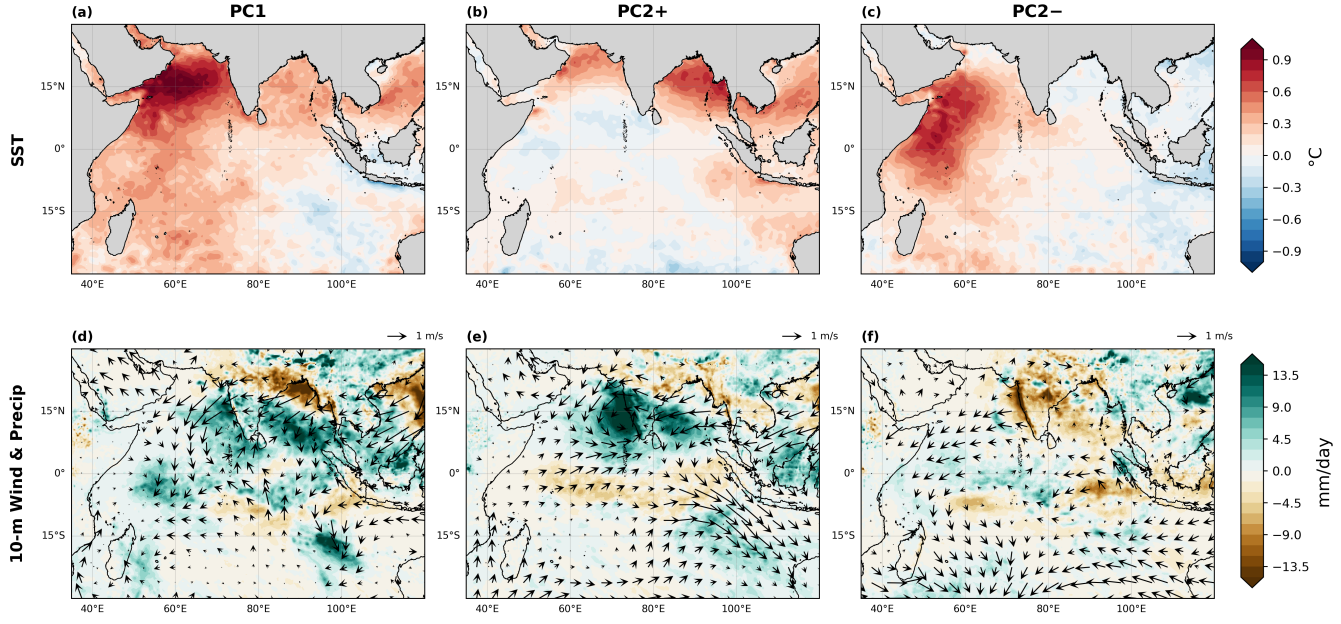

Figure 4. Composite anomalies of (top row) SST (°C) and (bottom row) precipitation (shading; mm/day) and 10-meter wind vectors (arrows; m/s) during MHW events associated with PC1 (left), PC2+ (middle), and PC2- (right) phases.

by cyclonic wind anomalies over the southeastern Arabian Sea and enhanced rainfall over southern India and the eastern Arabian Sea (Figure 4e). This is in agreement with Saranya et al. (2022), which shows that the MHW in the Bay of Bengal is associated with enhanced rainfall over southwest India. Compared to PC1, the rainfall anomalies are more intense but spatially concentrated, especially over the southern part of India. The negative of this mode is characterized by pronounced SST anomalies in the western Indian Ocean (Figure 4c), weak winds over the region, and widespread dry anomalies across India (Figure 4f). Unlike the previous two modes, this phase is associated with suppress monsoon activity across much of the Indian Subcontinent, likely due to weakened low-level monsoon circulation and absence of moisture convergence.

4.2 Atmospheric Conditions before the Marine Heatwaves

To understand the mechanisms driving these MHW events, we performed a composite analysis of atmospheric conditions during the five days prior to each MHW event for the three selected EOF modes (Figure 5). The variables include MSLP, surface wind, surface latent heat flux (positive downward), shortwave radiation flux (positive downward), and precipitation. Sensible heat flux and longwave radiation contributions to PC1 and PC2 (see composite maps in Fig. S3), are much smaller (by an order of magnitude) as compared with both shortwave radiation and latent heat flux contributions.

For the PC1 mode, a strong positive anomalous MSLP is observed to the north of the Arabian Sea, Indian subcontinent, Bay of Bengal, and northwest Pacific, while a corresponding negative anomaly appears in the southern Indian Ocean (Figure 5a). This pattern is detrimental to the summer monsoon flow, which is driven by a pressure gradient: high pressure over the Indian

https://doi.org/10.5194/egusphere-2025-3886
Preprint. Discussion started: 9 September 2025

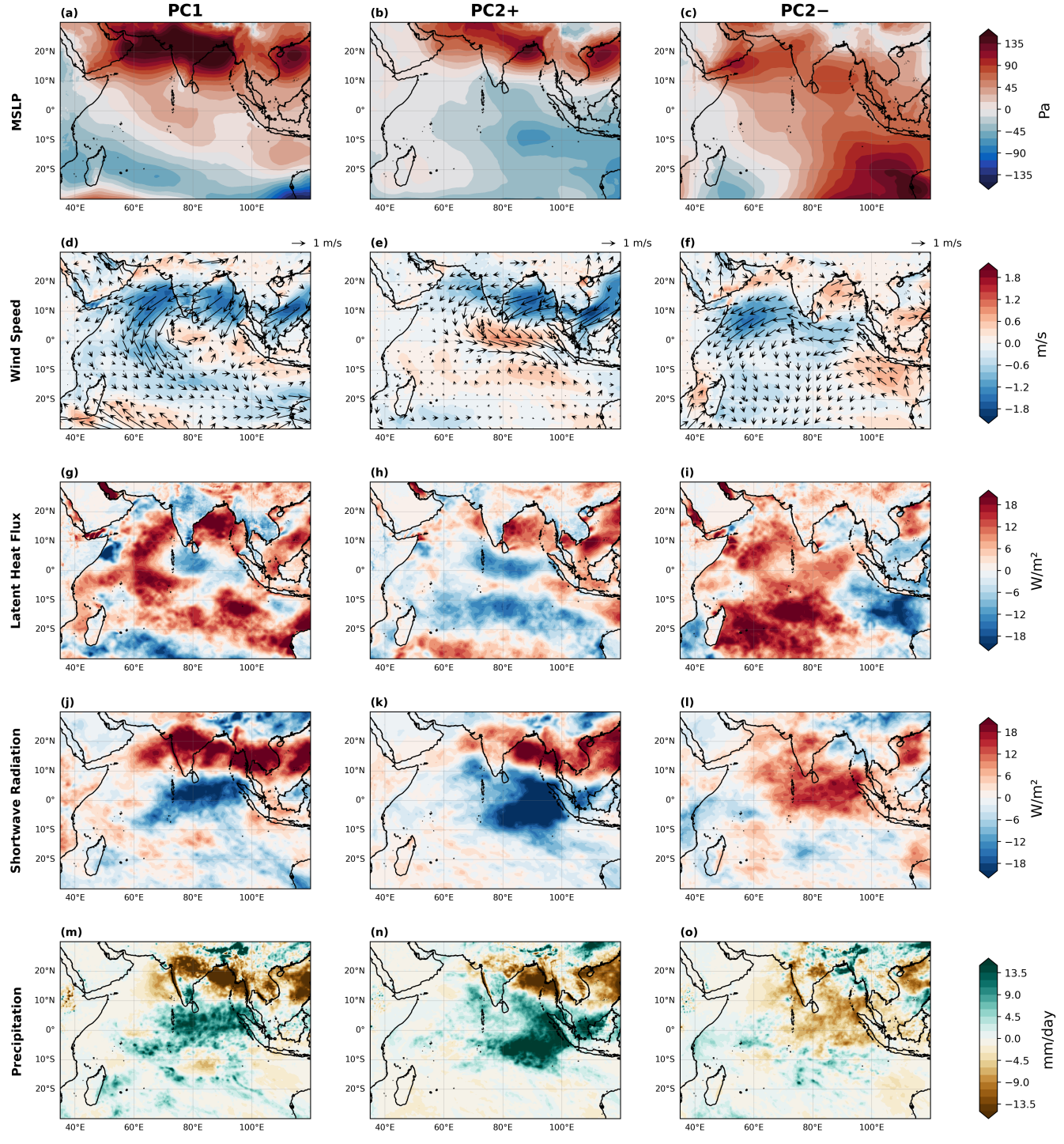

Figure 5. Composite anomalies averaged over the 5 days preceding MHW onset for the PC1 mode (left), PC2+ mode (middle), and PC2- mode (right). Rows show: (1) mean sea level pressure anomaly (Pa), (2) 10-meter wind speed anomaly (shading, m/s) and wind vector anomalies, (3) latent heat flux anomaly (W/m^2; positive downward), (4) shortwave radiation anomaly (W/m^2; positive downward), and (5) precipitation anomaly (mm/day).

https://doi.org/10.5194/egusphere-2025-3886
Preprint. Discussion started: 9 September 2025

Ocean and low pressure over the Indian subcontinent. As a result, these anomalies weaken the meridional pressure gradient and reduce the strength of southwesterly monsoon winds, as evident in the weakened cross-equatorial wind flow (Figure 5d). The weakening of surface winds reduces evaporation, which is reflected in the decreased upward latent heat flux (positive downwards) from the ocean to the atmosphere (Figure 5g). Lower evaporation rates could lead to fewer clouds (Fig. S4), allowing more incoming shortwave radiation to reach the ocean surface (Figure 5j). This radiative forcing, combined with reduced air-sea turbulent heat fluxes to the atmosphere, in turn driven by reduced winds, further enhances upper-ocean warming. The weaker winds can also reduce the wind-driven upper ocean mixing and have the potential to contribute to the ocean warming. The precipitation pattern shows dry conditions over western and central India and north of the Bay of Bengal, and wet conditions in the eastern equatorial Indian Ocean.

The atmospheric precursors of PC2+ mode MHWs also feature a reversal in the monsoon pressure gradient but with more localized intensity over the Bay of Bengal. Strong positive sea-level pressure anomalies are centered over the northern Bay of Bengal and the northwest Pacific, while a deep low persists over the southeastern Indian Ocean (Figure 5b). Compared to PC1, the gradient is sharper in the eastern basin, leading to more pronounced weakening of surface winds over the Bay of Bengal (Figure 5e). This suppresses evaporation and upward latent heat flux, inducing lower cloud cover and, in turn, increased solar radiation to enhance warming of the upper ocean (Figures 5h and k). The spatial confinement of this air-sea feedback (particularly the latent and shortwave flux) over the Bay of Bengal explains the eastward focus of MHWs in this mode. The precipitation pattern shows dry conditions north of the Bay of Bengal and wet conditions in the eastern equatorial Indian Ocean (Figure 5n).

For the PC2- mode, the composite atmospheric anomalies reveal a distinct pressure structure. Elevated MSLP anomalies appear entirely over the north Indian Ocean, with high values over the eastern Arabian Sea near the Gulf region, with a corresponding low in the southwestern Indian Ocean (Figure 5c). This configuration again opposes the typical monsoon pressure gradient, weakening the cross-equatorial winds, this time primarily over the western basin (Figure 5f). Reduced wind speeds lead to suppressed evaporation and latent heat loss (Figure 5i), consistent with sea surface warming. However, unlike the other modes, there is no substantial enhancement in shortwave radiation in this region, suggesting that MHW formation here is primarily driven by suppressed turbulent cooling rather than radiative forcing (Figure 5l). Furthermore, the weakening of nearshore winds along the Somali coast in the western Indian Ocean can suppress upwelling, thereby having the potential to reduce upwelling-induced cooling and contribute to elevated SSTs in the region. The precipitation anomaly shows dry conditions throughout India (Figure 5o).

4.3 Evolution of Atmospheric Drivers and SST leading to the Marine Heatwaves

The evolution of SST and atmospheric variables across the MHW hotspot regions relative to MHW onset is shown in Figure 6. For the PC1 mode, SST anomalies begin to emerge roughly eight days prior to the MHW onset (Figure 6a), following an early weakening of the meridional MSLP gradient (calculated as the meridional difference between 30°S–20°S and 10°N–20°N, averaged along the same longitude), starting up to 16 days before onset and becoming pronounced around 8 days before the onset (Figure 6b). Wind speeds decline in parallel, further reducing surface evaporation (Figure 6c). Latent heat flux anomalies

https://doi.org/10.5194/egusphere-2025-3886
Preprint. Discussion started: 9 September 2025

peak 6 days prior (Figure6d), consistent with diminished turbulent cooling. Meanwhile, shortwave radiation increases steadily, peaking before onset and staying elevated afterward (Figure 6e). The correlation analysis between key variables supports this hypothesis. A strong positive correlation is observed between MSLP and wind speed (r = 0.9 at lag 0), while wind speed and latent heat flux exhibit a strong negative correlation (r = –0.8 at lag 0). Additionally, latent heat flux is strongly correlated with shortwave radiation (r = 0.9). Shortwave radiation and SST show a significant positive correlation (r = 0.8) with a lag of 5 days. Moreover, SST demonstrates similarly high correlations with other variables, including MSLP, wind speed, and latent heat flux, all with a lag of 5 days, highlighting their potential roles in modulating SST variability.

For the Bay of Bengal (8°–25°N, 75°–100°E), PC2+ MHW events are preceded by a distinct atmospheric evolution (Figure 6). SST anomalies begin to develop just four days before onset (Figure 6a), while the MSLP gradient (calculated as the meridional difference between 5°S–15°S and 15°N–25°N, averaged along the same longitude) weakens over a longer window, starting 20 days prior to the onset, with a marked decline beginning nine days before (Figure6b). Wind speed anomalies sharply drop in this period (Figure 6c), triggering suppressed latent heat loss that peaks around four days before onset (Figure 6d). Shortwave radiation intensifies steadily (Figure 6e), with a magnitude similar to that of the latent heat flux anomaly. While the sequence mirrors PC1, the atmospheric anomalies are stronger and more localized over the Bay of Bengal, reinforcing the regional intensity and structure of PC2-positive events.

The evolution of drivers for PC2- events focused on the western Indian Ocean (10°S–15°N, 40°–65°E), shows subtle yet important distinctions (Figure 6). SST anomalies begin building as early as 16 days prior to MHW onset (Figure 6a), with weakening of the MSLP gradient observed from around 2 weeks prior to the onset (Figure 6b). Wind speeds begin a slower, more gradual decline from 18 days before onset (Figure 6c), leading to reduced evaporation and an increase in latent heat flux anomalies peaking four days before onset (Figure 6d). Shortwave radiation anomalies rise but remain relatively moderate and even dip a few days before the onset (Figure 6e). Unlike the other two modes, turbulent heat contributions are higher compared to the radiative heating, suggesting a dominance of the latent heat component (and plausibly reduced upwelling, as discussed in the previous section) in driving this mode.

5 The Post-Marine Heatwaves Impact on the Summer Monsoon Rainfall

The composite of key atmospheric variables averaged over five days following the MHW end dates (Figure 7), reveals contrasting patterns compared to those observed prior to the MHW events, with enhanced rainfall over the Indian Subcontinent. For the PC1 mode, negative pressure anomalies are evident over the North Indian Ocean, particularly over the Arabian Sea (Figure 7a). High SSTs during MHWs can slowly heat the air immediately above the ocean surface, increasing air temperature. This warmer air becomes less dense and rises, leading to divergence at higher altitudes. By mass continuity, this upward motion induces a decrease in surface pressure. The time lag between warm air rising and upper-level divergence is important to account for when explaining the impact of MHWs on atmospheric variables a few days later. The regression analysis between SST and MSLP during the MHW days for the three different modes shows negative values across most of the North Indian Ocean, indicating that SST and MSLP are inversely related (Fig. S9). This reduction in anomalous pressure helps strengthen

https://doi.org/10.5194/egusphere-2025-3886
Preprint. Discussion started: 9 September 2025

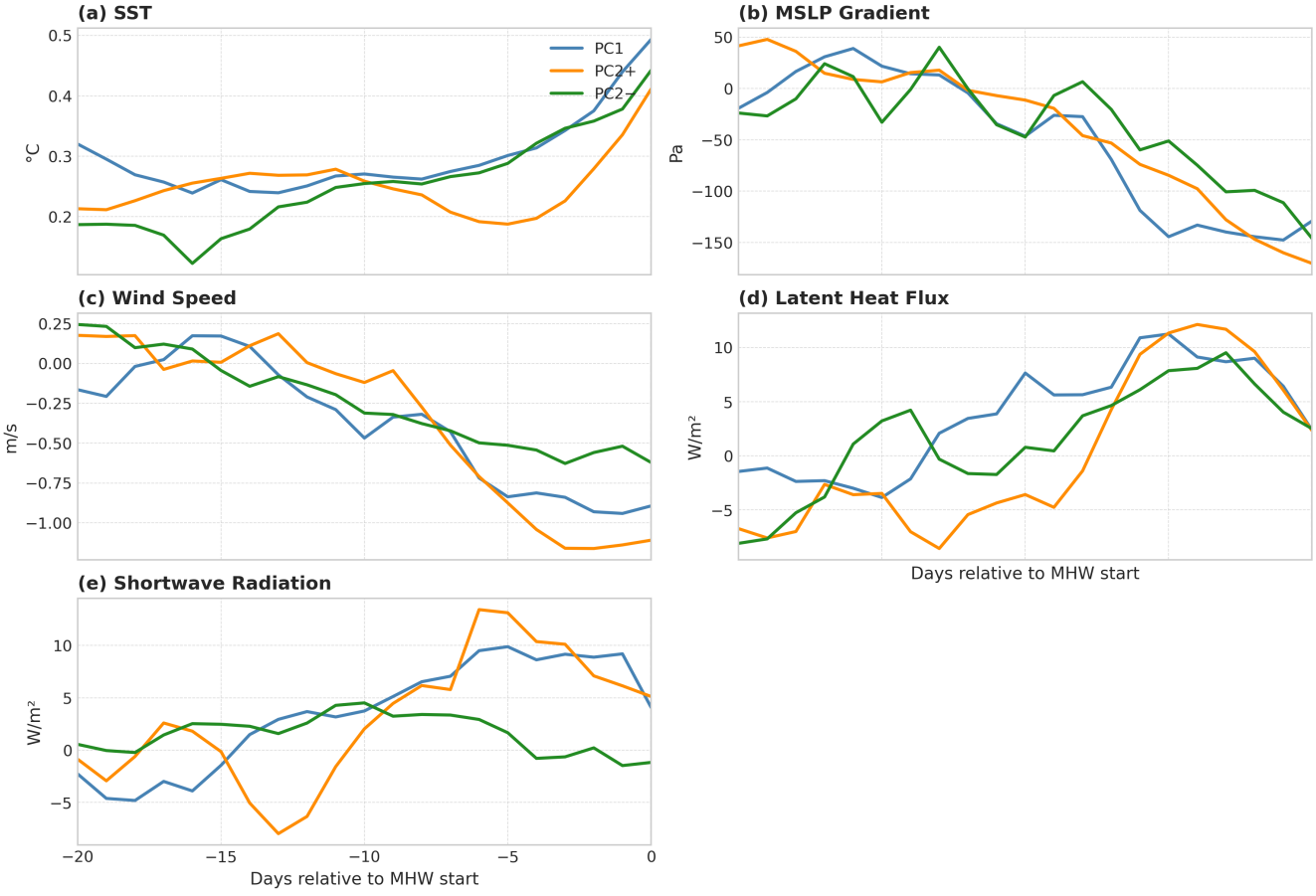

Figure 6. Time series of composite anomalies associated with MHW onset in the North Indian Ocean for PC1 (blue), PC2+ (orange), and PC2- (green) modes. Spatial means were computed over different domains: PC1 over 8°–25°N, 50°–100°E; PC2-positive over 8°–25°N, 75°–100°E; and PC2-negative over 10°S–15°N, 40°–65°E. For panel (b), the mean sea level pressure gradient was calculated for each mode as the meridional difference between the southern and northern bands: PC1: 10°S–20°S and 20°–30°N (averaged over 50°–100°E), PC2-positive: 5°S–15°S and 15°–25°N (averaged over 75°–100°E), and PC2-negative: 20°S–30°S and 10°–20°N (averaged over 40°–65°E). (a) Sea surface temperature anomaly (°C). (b) Mean sea level pressure gradient anomaly (Pa). (c) 10-meter wind speed anomaly (m/s). (d) Latent heat flux anomaly (W/m^2; positive downward). (e) Shortwave radiation anomaly (W/m^2; positive downward). Day 0 corresponds to the MHW onset date.

https://doi.org/10.5194/egusphere-2025-3886
Preprint. Discussion started: 9 September 2025

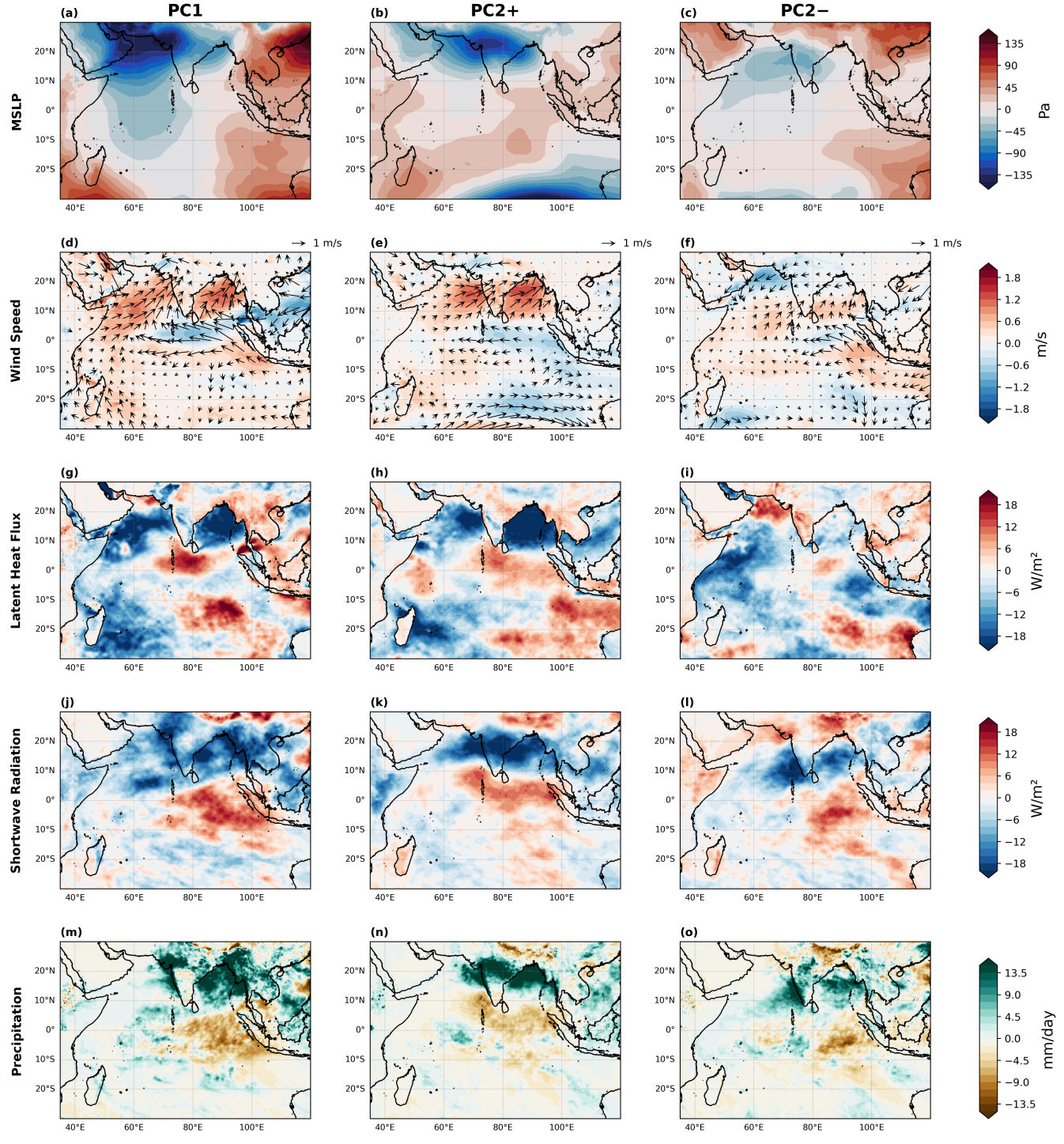

Figure 7. Composite anomalies averaged over the 5 days following MHW termination for the PC1 mode (left), PC2+ mode (middle), and PC2- mode (right). Rows show: (1) mean sea level pressure anomaly (Pa), (2) 10-meter wind speed anomaly (shading, m/s) and wind vector anomalies, (3) latent heat flux anomaly (W/m^2; positive downward), (4) shortwave radiation anomaly (W/m^2; positive downward), and (5) precipitation anomaly (mm/day).

https://doi.org/10.5194/egusphere-2025-3886
Preprint. Discussion started: 9 September 2025

the climatological monsoon pressure gradient, characterized by low pressure over the Indian subcontinent and high pressure over the southern Indian Ocean, which, in turn, enhances the monsoon circulation (Figure 7d). These strengthened winds promote increased evaporation over the ocean, as reflected in the negative latent heat flux anomalies (Figure 7g), indicating more heat being transferred from the ocean (which was stored during the MHW event) to the atmosphere. This enhanced evaporation also supports greater cloud formation, which in turn limits the amount of incoming solar radiation reaching the ocean surface (Figure 7j). As a result, the ocean loses heat both through latent heat flux and reduced radiative input, helping to terminate the MHW event. These post-MHW atmospheric adjustments are accompanied by enhanced precipitation over western and northeastern India, Bangladesh, Myanmar, and the Bay of Bengal region (Figure 7m). The increased evaporation over the Arabian Sea possibly contributes to greater moisture availability, which is subsequently transported toward western and central India. Similarly, elevated evaporation over the Bay of Bengal possibly enhances moisture convergence over northeastern India, Myanmar, Bangladesh, and the Bay of Bengal. This spatial pattern suggests a potential feedback mechanism, wherein MHW-induced ocean–atmosphere interactions can amplify monsoon rainfall following the decay of a basin-wide MHW event.

Post-event atmospheric anomalies for PC2+ MHWs closely resemble the recovery seen in PC1. A negative MSLP anomaly persists over the Bay of Bengal, central India, and the Arabian Sea (Figure 7b), enhancing the meridional pressure gradient and reviving monsoon winds across both basins (Figure 7e). These stronger winds increase latent heat release (Figure 7h) and cloud formation, which acts to reduce incoming shortwave radiation (Figure 7k). The combination of turbulent and radiative heat loss contributes to the decay of warm anomalies in the Bay of Bengal, terminating the MHW phase. Following PC2+ MHW events, precipitation intensifies primarily over central India and the northern Bay of Bengal (Figure 7n). Increased evaporation from both basins enhances atmospheric moisture, which then converges over these regions.

The termination phase of PC2- MHWs displays some differences. A broad negative pressure anomaly forms over central India and the Arabian Sea (Figure 7c), strengthening monsoon flow particularly in the southern Arabian Sea and across southern India (Figure 7f). However, winds remain weak over the northern Arabian Sea and north India, generating an anomalous cyclonic pattern over the subcontinent. In the southern basin, increased evaporation (Figure 7i) and diminished shortwave radiation (Figure 7l) accelerate ocean heat loss. Post-event rainfall anomalies for PC2-negative events are concentrated over southern and central India, as well as parts of the Bay of Bengal, which are the regions influenced by an anomalous cyclonic circulation (Figure 7o). Moisture buildup from enhanced evaporation in the western Indian Ocean likely fuels this rainfall response. While the overall feedback resembles that of the other modes, the southward shift in rainfall highlights the spatial sensitivity of monsoon response to MHW positioning and termination dynamics.

6 Monsoon Intraseasonal Oscillation and the Marine Heatwaves

The monsoon undergoes intraseasonal oscillations from May to October, known as the Monsoon Intraseasonal Oscillation (MISO) (Goswami and Mohan, 2001; Rajeevan et al., 2010). These oscillations includes active (wet) and break (dry) phases, typically lasting several days. MISO phases are derived using Extended Empirical Orthogonal Function analysis (Suhas et al., 2012). Composite anomalies of precipitation and MSLP during the eight MISO phases, computed using the ERA5 rainfall

https://doi.org/10.5194/egusphere-2025-3886
Preprint. Discussion started: 9 September 2025

data (see Fig. S5 and Fig. S6), align with those shown by Suhas et al. (2012) using IMD data. For example, during MISO Phase 1, enhanced convection is centered near the equator, which then migrates northward over subsequent phases. Similarly, an anomalous high-pressure center is seen over the Indian subcontinent during the initial four phases, transitioning to low pressure in the later phases. Interestingly, some of these MISO composite patterns resemble the pre-MHW conditions seen in different EOF modes of MHWs. For example, the precipitation anomaly patterns during PC1 and PC2+ (see Figures 4) are similar to those during MISO Phase 3, where enhanced convection is concentrated over the southern Indian Ocean and Bay of Bengal, with suppressed rainfall over central India and the northern Bay of Bengal. Likewise, the MSLP and precipitation anomalies observed five days prior to MHW onset (Figures 5) resemble those seen during MISO Phase 3 (Fig. S5 and Fig. S6).

To examine the interaction between MISO and MHWs more systematically, we analyzed the daily percentage occurrence of each MISO phase from 10 days before to 10 days after MHW onset for events in each EOF mode (Figure 8). In Mode 1, we observe a sequential transition from MISO Phase 1 (centered around day -10) to Phase 3 (around day 0), followed by a scattered distribution of Phases 4 and 5 after the onset. This suggests a potential link between the early MISO phases and the buildup toward MHW events in PC1. The progression is more coherent in PC2+, where a clear temporal propagation from Phase 1 through Phase 5 is visible from day -10 to day 10. Particularly, Phase 2 and Phase 3 dominate in the days immediately leading up to MHW onset (with occurrence frequencies exceeding 30%), followed by the transition to Phases 4 and 5 in the post-onset days. This indicates that MHWs of PC2+ often arise during initial MISO events. In contrast, the PC2- panel displays a very different pattern. Here, MISO Phases 6 to 8 dominate around the MHW onset, peaking on days -3 to +1. This suggests that PC2- MHWs are more likely to form during later phases of MISO.

These findings suggest a possible influence of MISO conditions on MHW variability in the North Indian Ocean. Specifically, PC1 MHWs often occur during El Niño years and align with MISO Phase 3, PC2+ with La Niña years and MISO Phase 3, and Mode 2-negative with El Niño years and MISO Phase 8.

7 Summary and Discussion

Our planet is warming rapidly, and with it, the frequency and intensity of MHWs are also increasing. MHWs are typically defined as periods when daily SST anomalies exceed the seasonally varying 90th percentile threshold, calculated using a fixed climatology, for five or more consecutive days. However, recent studies have indicated that using a fixed baseline can artificially raise the observed increase in MHW frequency as global SSTs rise, effectively making the "unusual" the "new normal." To address this issue, we defined MHWs using detrended SST anomalies, thereby isolating internal variability from long-term warming, and investigated the variability, drivers, and monsoon impacts of MHWs in the North Indian Ocean.

An EOF analysis of MHW intensity revealed two dominant modes of variability. The first mode, explaining 22% of the total variance, shows basin-wide MHWs with particularly strong signals in the Arabian Sea. This mode is linked to an anomalous high pressure over the North Indian Ocean and a corresponding low pressure in the Southern Hemisphere. This configuration weakens the climatological pressure gradient and hence the monsoon winds, which in turn suppresses evaporation (and hence

https://doi.org/10.5194/egusphere-2025-3886
Preprint. Discussion started: 9 September 2025

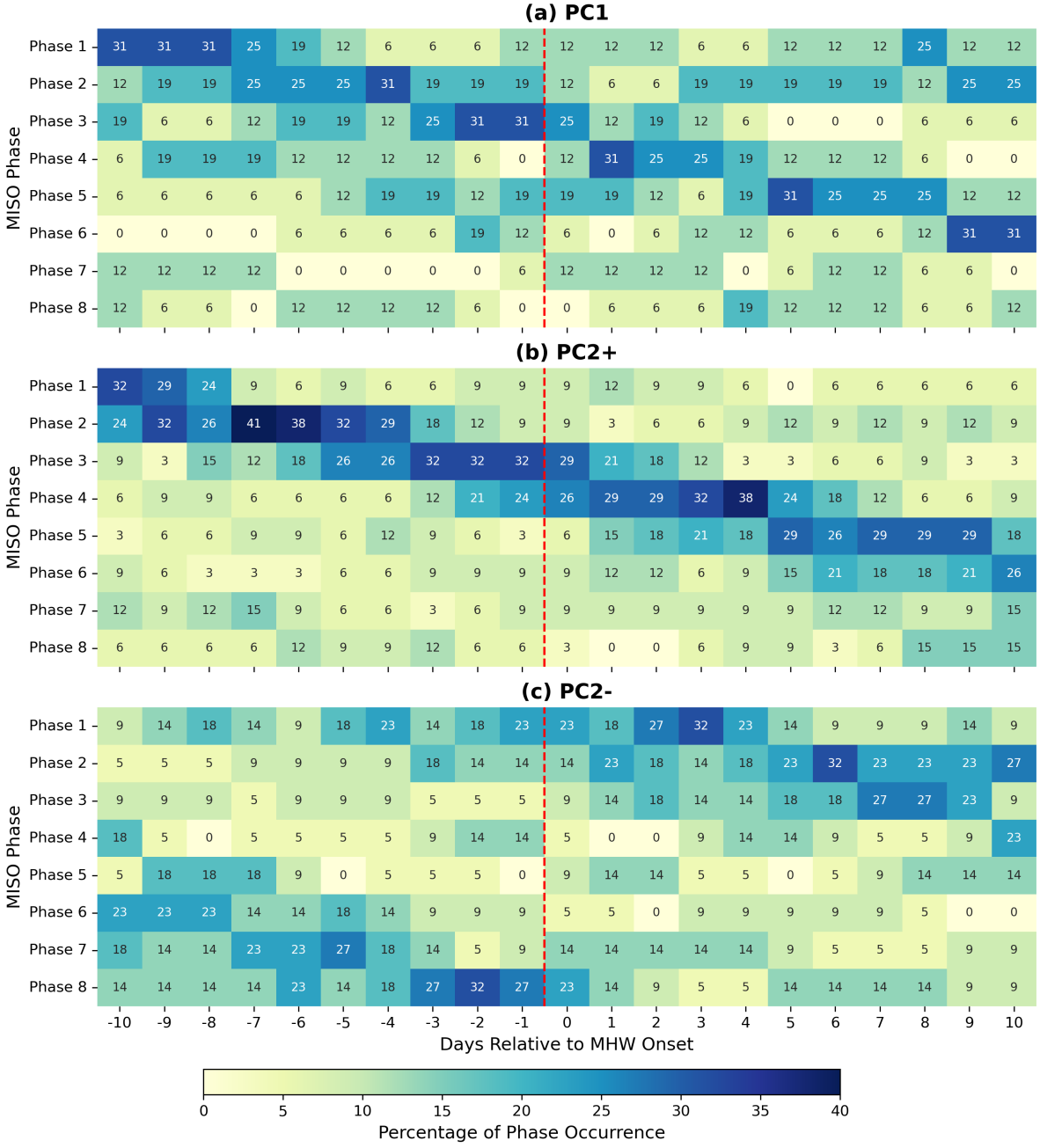

Figure 8. Daily percentage of MISO phase occurrences from 10 days before to 10 days after MHW onset (day 0), computed across all events in each category: (a) PC1, (b) PC2+, and (c) PC2-. For each day relative to MHW onset, the percentage reflects the frequency with which each MISO phase occurred, normalized by the total number of events on that day. The red dashed line indicates the day of MHW onset (day 0).

https://doi.org/10.5194/egusphere-2025-3886
Preprint. Discussion started: 9 September 2025

reducing evaporative cooling) and cloud formation. As a result, shortwave radiation penetrates more effectively, warming the upper ocean and promoting MHWs (Figure 5). The second mode, accounting for 8% of the total variance, shows a dipole-like pattern where its positive phase is characterized by MHWs in the Bay of Bengal and suppressed activity in the Arabian Sea, while the negative phase exhibits the opposite pattern. The positive phase is driven by mechanisms similar to EOF mode 1, though the effects are more localized over the Bay of Bengal. In the negative phase, MHWs are concentrated over the western Indian Ocean, particularly near the Somali coast. In this case, the weakening of monsoon winds is also confined to the region, potentially reducing upwelling and the associated cooling, thereby allowing SSTs to rise. Interestingly, shortwave radiation appears to play a less dominant role in this mode compared to the others.

We further found that natural climate variability on different timescales significantly modulates MHW occurrence in the North Indian Ocean. For example, during El Niño years, SSTs are anomalously high across the north Indian Ocean basin, with particularly intense warming in the Arabian Sea (see Fig. S7). Meanwhile, inactive phases of MISO, which is characterized by weaker monsoon winds, reduce evaporative cooling and cloud formation, allowing more shortwave radiation to warm the upper ocean. When El Niño conditions coincide with an inactive MISO phase, they can reinforce each other, leading to basin-wide MHW consistent with PC1 mode. Conversely, during La Niña years, the western Indian Ocean tends to be cooler overall, but anomalously low pressure prevails across much of the northern Indian Ocean and adjacent landmasses, except over the northern Bay of Bengal and northeastern India, where pressure is anomalously high (see Fig. S8). Low-level winds are typically weaker over the Bay of Bengal relative to the Arabian Sea under La Niña conditions (see Fig. S8). If an inactive MISO phase occurs simultaneously, it further weakens monsoon winds and increases pressure over the Bay of Bengal. The combined effect can amplify high-pressure anomalies over the northern Bay of Bengal and surrounding regions, resulting in localized MHW development in the Bay of Bengal consistent with the positive phase of EOF mode 2.

These different EOF modes also modulate monsoon rainfall in distinct ways. During the positive phases of PC1 and PC2, southern India tends to experience wetter conditions, while northern India becomes relatively drier, a rainfall distribution commonly associated with MISO phases 3–4. In contrast, PC2- is linked to widespread dryness across much of the Indian subcontinent. We also investigated the post-MHW rainfall response and found that the termination of PC1 events typically brings enhanced rainfall to northwest and northeast India, as well as to Bangladesh and Myanmar. In contrast, the end of PC2+ events is followed by increased rainfall over central India, while PC2- termination leads to enhanced rainfall over both south and central India. These delayed impacts are likely driven by the revival of monsoon winds following a break phase, which promotes the release of oceanic heat and moisture stored during the MHW event. These strengthened winds enhance evaporation over the ocean, as evidenced by negative latent heat flux anomalies, indicating heat transfer from ocean to atmosphere. The associated moisture flux contributes to increased cloud formation, which can further reduce incoming solar radiation, stabilizing the ocean surface and reinforcing the transition toward wetter atmospheric conditions.

Our findings are consistent with the mechanisms highlighted by Roxy et al. (2017), who showed that SST warming in the Arabian Sea and the Bay of Bengal plays a critical role in fueling extreme rainfall events over central India. They traced nearly 36% of the total moisture during such events to the Arabian Sea, more than from the Bay of Bengal (26%) and central Indian Ocean (9%) combined. This underscores the importance of SST anomalies, such as those during MHWs, as a key

https://doi.org/10.5194/egusphere-2025-3886
Preprint. Discussion started: 9 September 2025

moisture source. Additionally, a statistically significant increase in Arabian Sea moisture contribution has been observed over recent decades, suggesting a growing role for oceanic heat events like MHWs in intensifying monsoon extremes under climate change.

Overall, this study underscores the critical role of both the spatial structure and timing of MHWs in shaping monsoon variability. The results have significant implications for understanding and predicting regional rainfall extremes in a warming climate. Previous studies have shown that warming of the western Indian Ocean tends to reduce rainfall over the Indian subcontinent by weakening the land–sea pressure gradient and associated monsoon winds (Roxy et al., 2015). In contrast, our results suggest that Indian Ocean warming, particularly through marine heatwaves, can enhance precipitation over parts of South Asia by increasing evaporation. Moreover, our findings suggest a possible interaction between MHWs and the MISO, raising important directions for future research. Several studies have shown that the air-sea interactions can influence the MISO precipitation (ROXY and TANIMOTO, 2007; Ajayamohan et al., 2008; Wang et al., 2009; Lin et al., 2010; Sabeerali et al., 2014). Therefore, key questions include: Do MHWs feed back onto MISO by modulating SST and atmospheric convection? Can MHWs alter the propagation speed or intensity of MISO phases? Do MHWs shift the canonical rainfall patterns associated with different MISO phases? Could they delay or accelerate MISO phase transitions? How do larger-scale modes such as ENSO and the IOD modulate the MISO–MHW relationship? While these questions lie beyond the scope of the present study, they open up new directions for advancing our understanding of ocean–atmosphere coupling and improving monsoon forecasting skill in a changing climate. In particular, since we define MHWs using detrended SST anomalies, future research could investigate whether similar MHW–MISO interactions persist when using raw SSTs that include long-term warming trends.

Data availability. The ERA5 data set used in this study is available to download from https://cds.climate.copernicus.eu/ (Hersbach et al., 2020). The OISST data is available to download at https://psl.noaa.gov/data/gridded/data.noaa.oisst.v2.highres.html. The Niño 3.4 and DMI monthly time series are available to download at https://psl.noaa.gov/data/timeseries/month/.

Code and data availability. Figures shown in this study are plotted using Python (https://www.python.org/). Codes can be obtained from the corresponding author.

Author contributions. LJ: Conceptualization, Formal Analysis, Investigation, Methodology, Supervision, Validation, Visualization, Writing-original draft, Writing-review & editing; NS: Conceptualization, Methodology, Supervision, Validation, Writing-review & editing; VS: Conceptualization, Investigation, Methodology, Validation, Writing-review & editing; DD: Conceptualization, Investigation, Methodology, Validation, Writing-review & editing; RM: Supervision, Validation, Writing-review & editing

https://doi.org/10.5194/egusphere-2025-3886
Preprint. Discussion started: 9 September 2025

Disclaimer. The boundaries and names shown (if any) on the maps in this study are for illustrative purposes only and do not imply any opinion on the part of the authors concerning the legal status of any country, territory, or area, or concerning the delimitation of its frontiers or boundaries.

Competing interests. The corresponding author has declared that none of the authors has any competing interests.

Acknowledgements. This work was supported by the Natural Environment Research Council [Grant NE/S007210/1]. DD is supported by the IIT Bhubaneswar seed grant [Grant RP426]. The authors gratefully acknowledge Lijo Abraham Joseph for his valuable discussions and insights. AI tools such as ChatGPT and Grammarly were occasionally and mindfully used to assist with writing refinement and Python code refinement. This research also utilized JASMIN, the UK's collaborative data analysis facility.

https://doi.org/10.5194/egusphere-2025-3886
Preprint. Discussion started: 9 September 2025

References

Ajayamohan, R. S., Rao, S. A., and Yamagata, T.: Influence of Indian Ocean Dipole on Poleward Propagation of Boreal Summer Intraseasonal Oscillations, Journal of Climate, 21, 5437–5454, https://doi.org/10.1175/2008jcli1758.1, 2008.

Albert, J., Gulakaram, V. S., Vissa, N. K., Bhaskaran, P. K., and Dash, M. K.: Recent Warming Trends in the Arabian Sea: Causative Factors and Physical Mechanisms, Climate, 11, 35–35, https://doi.org/10.3390/cli11020035, 2023.

Amaya, D. J., Jacox, M. G., Fewings, M. R., Saba, V. S., Stuecker, M. F., Rykaczewski, R. R., Ross, A. C., Stock, C. A., Capotondi, A., Petrik, C. M., Bograd, S. J., Alexander, M. A., Cheng, W., Hermann, A. J., Kearney, K. A., and Powell, B. S.: Marine heatwaves need clear definitions so coastal communities can adapt, Nature, 616, 29–32, 2023.

Capotondi, A., Rodrigues, R. R., Sen Gupta, A., Benthuysen, J. A., Deser, C., Frölicher, T. L., Lovenduski, N. S., Amaya, D. J., Le Grix, N., Xu, T., Hermes, J., Holbrook, N. J., Martinez-Villalobos, C., Masina, S., Roxy, M. K., Schaeffer, A., Schlegel, R. W., Smith, K. E., and Wang, C.: A global overview of marine heatwaves in a changing climate, Commun. Earth Environ., 5, 2024.

Chakraborty, A., Chandrakar, R., Kumar, S., Sadhukhan, B., and Kumar, A.: Analysis of marine heatwaves and biogeochemistry in the Northern Arabian Sea, Reg. Stud. Mar. Sci., 63, 103 019, 2023.

Chatterjee, A., Anil, G., and Shenoy, L. R.: Marine heatwaves in the Arabian Sea, Ocean Sci., 18, 639–657, 2022.

Chatterjee, A., Sajidh, C. K., Murtugudde, R., McPhaden, M. J., Shenoi, S. S. C., and Vinayachandran, P. N.: Rapid 21st century warming in the Southern Indian Ocean driven by altered inter-basin connections, https://doi.org/10.21203/rs.3.rs-4247247/v1, 2024.

Cheng, Y., Zhang, M., Song, Z., Wang, G., Zhao, C., Shu, Q., Zhang, Y., and Qiao, F.: A quantitative analysis of marine heatwaves in response to rising sea surface temperature, Sci. Total Environ., 881, 163 396, 2023.

Dey, D. and Döös, K.: Tracing the Origin of the South Asian Summer Monsoon Precipitation and Its Variability Using a Novel Lagrangian Framework, Journal of Climate, 34, 8655 – 8668, https://doi.org/10.1175/JCLI-D-20-0967.1, 2021.

D'Mello, J. R. and Kumar, S. P.: Processes controlling the accelerated warming of the Arabian Sea, International Journal of Climatology, 38, 1074–1086, https://doi.org/10.1002/JOC.5198, 2018.

Gao, X., Li, G., Liu, J., and Long, S.-M.: The Trend and Interannual Variability of Marine Heatwaves over the Bay of Bengal, Atmosphere, 13, 469, https://doi.org/10.3390/atmos13030469, 2022.

Good, S., Fiedler, E., Mao, C., Martin, M. J., Maycock, A., Reid, R., Roberts-Jones, J., Searle, T., Waters, J., While, J., and Worsfold, M.: The Current Configuration of the OSTIA System for Operational Production of Foundation Sea Surface Temperature and Ice Concentration Analyses, Remote Sensing, 12, 720, https://doi.org/10.3390/rs12040720, 2020.

Goswami, B. N. and Mohan, R. S. A.: Intraseasonal Oscillations and Interannual Variability of the Indian Summer Monsoon, Journal of Climate, 14, 1180–1198, https://doi.org/10.1175/1520-0442(2001)014<1180:ioaivo>2.0.co;2, 2001.

Guo, F., Liu, Q., Yang, J., and Fan, L.: Three types of Indian Ocean Basin modes, Climate Dynamics, 51, 4357–4370, https://doi.org/10.1007/s00382-017-3676-z, 2017.

Gupta, H., Sil, S., Gangopadhyay, A., and Gawarkiewicz, G.: Observed surface and subsurface Marine Heat Waves in the Bay of Bengal from in-situ and high-resolution satellite data, Climate Dynamics, 62, 203–221, https://doi.org/10.1007/s00382-023-06913-5, 2023.

Gupta, H., Deogharia, R., Sil, S., and Dey, D.: Characteristics of Marine Heat Extreme Evolution in the Northern Indian Ocean, International Journal of Climatology, 45, https://doi.org/10.1002/joc.8734, 2024.

Hersbach, H., Bell, B., Berrisford, P., Hirahara, S., Horányi, A., Muñoz-Sabater, J., Nicolas, J., Peubey, C., Radu, R., Schepers, D., Simmons, A., Soci, C., Abdalla, S., Abellan, X., Balsamo, G., Bechtold, P., Biavati, G., Bidlot, J., Bonavita, M., De Chiara, G., Dahlgren, P., Dee,

https://doi.org/10.5194/egusphere-2025-3886
Preprint. Discussion started: 9 September 2025

D., Diamantakis, M., Dragani, R., Flemming, J., Forbes, R., Fuentes, M., Geer, A., Haimberger, L., Healy, S., Hogan, R. J., Hólm, E., Janisková, M., Keeley, S., Laloyaux, P., Lopez, P., Lupu, C., Radnoti, G., de Rosnay, P., Rozum, I., Vamborg, F., Villaume, S., and Jean-Noël Thépaut: The ERA5 global reanalysis, Q. J. R. Meteorol. Soc., 146, 1999–2049, 2020.

Hobday, A. J., Alexander, L. V., Perkins, S. E., Smale, D. A., Straub, S. C., Oliver, E. C., Benthuysen, J. A., Burrows, M. T., Donat, M. G., Feng, M., Holbrook, N. J., Moore, P. J., Scannell, H. A., Sen Gupta, A., and Wernberg, T.: A hierarchical approach to defining marine heatwaves, Progress in Oceanography, 141, 227–238, https://doi.org/10.1016/j.pocean.2015.12.014, 2016.

Jacox, M. G.: Marine heatwaves in a changing climate, Nature, 571, 485–487, 2019.

Johnson, G. C., Lumpkin, R., Atkinson, C., Biló, T., Boyer, T., Bringas, F., Carter, B. R., Cetinić, I., Chambers, D. P., Chan, D., Cheng, L., Chomiak, L., Cronin, M. F., Dong, S., Feely, R. A., Franz, B. A., Gao, M., Garg, J., Gilson, J., Goni, G., Hamlington, B. D., Hobbs, W., Hu, Z.-Z., Huang, B., Ishii, M., Jevrejeva, S., Johns, W., Landschützer, P., Lankhorst, M., Leuliette, E., Locarnini, R., Lyman, J. M., McPhaden, M. J., Merrifield, M. A., Mishonov, A., Mitchum, G. T., Moat, B. I., Mrekaj, I., Nerem, R. S., Purkey, S. G., Qiu, B., Reagan, J., Sato, K., Schmid, C., Sharp, J. D., Siegel, D. A., Smeed, D. A., Stackhouse, P. W., Sweet, W., Thompson, P. R., Triñanes, J. A., Volkov, D. L., Wanninkhof, R., Wen, C., Westberry, T. K., Widlansky, M. J., Willis, J., Xie, P.-P., Yin, X., min Zhang, H., Zhang, L., Allen, J., Camper, A. V., Haley, B. O., Hammer, G., Love-Brotak, S. E., Ohlmann, L., Noguchi, L., Riddle, D. B., and Veasey, S. W.: Global Oceans, Bulletin of the American Meteorological Society, 104, S146 – S206, https://doi.org/10.1175/BAMS-D-23-0076.2, 2023.

Joseph, L., Skliris, N., Dey, D., Marsh, R., and Hirschi, J.: Increased Summer Monsoon Rainfall Over Northwest India Caused by Hadley Cell Expansion and Indian Ocean Warming, Geophysical Research Letters, 51, https://doi.org/10.1029/2024gl108829, 2024.

Joseph, L., Dey, D., Skliris, N., Sanchez-Franks, A., Marsh, R., Hirschi, J. J.-M., and Golla, S.: Advection-Driven Warming Trend in the Western Indian Ocean, Preprint, https://doi.org/10.22541/au.174526317.71272890/v1, 2025.

Klein, S. A., Soden, B. J., and Lau, N.-C.: Remote Sea Surface Temperature Variations during ENSO: Evidence for a Tropical Atmospheric Bridge, Journal of Climate, 12, 917–932, https://doi.org/10.1175/1520-0442(1999)012<0917:rsstvd>2.0.co;2, 1999.

Koul, V., Brune, S., Akimova, A., Düsterhus, A., Pieper, P., Hövel, L., Parekh, A., Schrum, C., and Baehr, J.: Seasonal prediction of Arabian Sea marine heatwaves, Geophys. Res. Lett., 50, 2023.

Kumar, S., Chakraborty, A., Chandrakar, R., Kumar, A., Sadhukhan, B., and Roy Chowdhury, R.: Analysis of marine heatwaves over the Bay of Bengal during 1982–2021, Scientific Reports, 13, https://doi.org/10.1038/s41598-023-39884-y, 2023.

Liang, K., Qiu, Y., Lin, X., Lin, W., Ni, X., and He, Y.: An Increase in Autumn Marine Heatwaves Caused by the Indian Ocean Dipole in the Bay of Bengal, Journal of Climate, 37, 4523–4539, https://doi.org/10.1175/jcli-d-23-0541.1, 2024.

Lin, A., Li, T., Fu, X., Luo, J.-J., and Masumoto, Y.: Effects of air–sea coupling on the boreal summer intraseasonal oscillations over the tropical Indian Ocean, Climate Dynamics, 37, 2303–2322, https://doi.org/10.1007/s00382-010-0943-7, 2010.

Mathew, S., Natesan, U., Latha, G., and Venkatesan, R.: Dynamics behind warming of the southeastern Arabian Sea and its interruption based on in situ measurements, Ocean Dynamics, 68, 457–467, https://doi.org/10.1007/S10236-018-1130-3, 2018.

McMonigal, K., Gunn, K. L., Beal, L. M., Elipot, S., and Willis, J. K.: Reduction in Meridional Heat Export Contributes to Recent Indian Ocean Warming, Journal of Physical Oceanography, 52, 329 – 345, https://doi.org/10.1175/JPO-D-21-0085.1, 2022.

Nisha, P., Pranesha, T., Vidya, P., Ravichandran, M., and Murtugudde, R.: Trend and interannual variability of the Arabian Sea heat content, Journal of Marine Systems, https://doi.org/10.1016/j.jmarsys.2023.103935, 2023.

Oliver, E. C. J., Donat, M. G., Burrows, M. T., Moore, P. J., Smale, D. A., Alexander, L. V., Benthuysen, J. A., Feng, M., Sen Gupta, A., Hobday, A. J., Holbrook, N. J., Perkins-Kirkpatrick, S. E., Scannell, H. A., Straub, S. C., and Wernberg, T.: Longer and more frequent marine heatwaves over the past century, Nat. Commun., 9, 2018.

https://doi.org/10.5194/egusphere-2025-3886
Preprint. Discussion started: 9 September 2025

Oppo, D. W. and Rosenthal, Y.: The Great Indo-Pacific Communicator, Science, 328, 1492–1494, https://doi.org/10.1126/SCIENCE.1187273, 2010.

Prajeesh, A. G., Swapna, P., Krishnan, R., Ayantika, D. C., Sandeep, N., Manmeet, S., Aditi, M., and Sandip, I.: The Indian summer monsoon and Indian Ocean Dipole connection in the IITM Earth System Model (IITM-ESM), Climate Dynamics, 58, 1877–1897, https://doi.org/10.1007/s00382-021-05999-z, 2021.

Pratik, K., Parekh, A., Karmakar, A., Chowdary, J. S., and Gnanaseelan, C.: Recent changes in the summer monsoon circulation and their impact on dynamics and thermodynamics of the Arabian Sea, Theoretical and Applied Climatology, 136, 321–331, https://doi.org/10.1007/s00704-018-2493-6, 2018.

Rajeevan, M., Gadgil, S., and Bhate, J.: Active and break spells of the Indian summer monsoon, Journal of Earth System Science, 119, 229–247, https://doi.org/10.1007/s12040-010-0019-4, 2010.

Rayner, N. A., Parker, D. E., Horton, E. B., Folland, C. K., Alexander, L. V., Rowell, D. P., Kent, E. C., and Kaplan, A.: Global analyses of sea surface temperature, sea ice, and night marine air temperature since the late nineteenth century, Journal of Geophysical Research: Atmospheres, 108, https://doi.org/10.1029/2002jd002670, 2003.

Reynolds, R. W., Rayner, N. A., Smith, T. M., Stokes, D. C., and Wang, W.: An Improved In Situ and Satellite SST Analysis for Climate, Journal of Climate, 15, 1609–1625, https://doi.org/10.1175/1520-0442(2002)015<1609:aiisas>2.0.co;2, 2002.

Rohde, R.: Global Temperature Report for 2024, https://berkeleyearth.org/global-temperature-report-for-2024/, accessed: 2025-05-21, 2025.

Rosselló, P., Pascual, A., and Combes, V.: Assessing marine heat waves in the Mediterranean Sea: a comparison of fixed and moving baseline methods, Front. Mar. Sci., 10, 2023.

ROXY, M. and TANIMOTO, Y.: Role of SST over the Indian Ocean in Influencing the Intraseasonal Variability of the Indian Summer Monsoon, Journal of the Meteorological Society of Japan. Ser. II, 85, 349–358, https://doi.org/10.2151/jmsj.85.349, 2007.

Roxy, M. K., Ritika, K., Terray, P., and Masson, S.: The Curious Case of Indian Ocean Warming, Journal of Climate, 27, 8501 – 8509, https://doi.org/10.1175/JCLI-D-14-00471.1, 2014.

Roxy, M. K., Ritika, K., Terray, P., Murtugudde, R., Ashok, K., and Goswami, B. N.: Drying of Indian subcontinent by rapid Indian Ocean warming and a weakening land-sea thermal gradient, Nature Communications, 6, https://doi.org/10.1038/ncomms8423, 2015.

Roxy, M. K., Ghosh, S., Pathak, A., Athulya, R., Mujumdar, M., Murtugudde, R., Terray, P., and Rajeevan, M.: A threefold rise in widespread extreme rain events over central India, Nature Communications, 8, https://doi.org/10.1038/s41467-017-00744-9, 2017.

Roxy, M. K., Saranya, J. S., Modi, A., Anusree, A., Cai, W., Resplandy, L., Vialard, J., and Frölicher, T. L.: Future projections for the tropical Indian Ocean, in: The Indian Ocean and its Role in the Global Climate System, pp. 469–482, Elsevier, 2024.

Sabeerali, C. T., Rao, S. A., George, G., Rao, D. N., Mahapatra, S., Kulkarni, A., and Murtugudde, R.: Modulation of monsoon intraseasonal oscillations in the recent warming period, Journal of Geophysical Research: Atmospheres, 119, 5185–5203, https://doi.org/10.1002/2013jd021261, 2014.

Saranya, J. S., Roxy, M. K., Dasgupta, P., and Anand, A.: Genesis and trends in marine heatwaves over the tropical Indian ocean and their interaction with the Indian summer monsoon, J. Geophys. Res. Oceans, 127, 2022.

Shee, A., Sil, S., and Gangopadhyay, A.: Recent changes in the upper oceanic water masses over the Indian Ocean using Argo data, Scientific Reports, 13, https://doi.org/10.1038/s41598-023-47658-9, 2023.

Skliris, N., Marsh, R., Haigh, I. D., Wood, M., Hirschi, J., Darby, S., Quynh, N. P., and Hung, N. N.: Drivers of rainfall trends in and around Mainland Southeast Asia, Frontiers in Climate, 4, https://doi.org/10.3389/fclim.2022.926568, 2022.

https://doi.org/10.5194/egusphere-2025-3886
Preprint. Discussion started: 9 September 2025

Suhas, E., Neena, J. M., and Goswami, B. N.: An Indian monsoon intraseasonal oscillations (MISO) index for real time monitoring and forecast verification, Climate Dynamics, 40, 2605–2616, https://doi.org/10.1007/s00382-012-1462-5, 2012.

Swapna, P., Krishnan, R., and Wallace, J. M.: Indian Ocean and monsoon coupled interactions in a warming environment, Climate Dynamics, 42, 2439–2454, https://doi.org/10.1007/s00382-013-1787-8, 2013.

Swetha, S., Ramesh, K. V., and Rakesh, V.: Influence of large-scale climate modes (ENSO, IOD and PJ) on marine heatwave characteristics in the Indian ocean region, Theoretical and Applied Climatology, 156, https://doi.org/10.1007/s00704-025-05570-4, 2025.

Titchner, H. A. and Rayner, N. A.: The Met Office Hadley Centre sea ice and sea surface temperature data set, version 2: 1. Sea ice concentrations: HADISST.2.1.0.0 SEA ICE CONCENTRATIONS, Journal of Geophysical Research: Atmospheres, 119, 2864–2889, https://doi.org/10.1002/2013jd020316, 2014.

Venegas, R. M., Acevedo, J., and Treml, E. A.: Three decades of ocean warming impacts on marine ecosystems: A review and perspective, Deep Sea Research Part II: Topical Studies in Oceanography, 212, 105 318, https://doi.org/https://doi.org/10.1016/j.dsr2.2023.105318, 2023.

Wang, W., Chen, M., and Kumar, A.: Impacts of Ocean Surface on the Northward Propagation of the Boreal Summer Intraseasonal Oscillation in the NCEP Climate Forecast System, Journal of Climate, 22, 6561–6576, https://doi.org/10.1175/2009jcli3007.1, 2009.

World Meteorological Organization: State of the Climate 2024: Update for COP29, https://library.wmo.int/idurl/4/69075, accessed: 2025-05-21, 2025.

Xie, S.-P., Hu, K., Hafner, J., Tokinaga, H., Du, Y., Huang, G., and Sampe, T.: Indian Ocean Capacitor Effect on Indo–Western Pacific Climate during the Summer following El Niño, Journal of Climate, 22, 730–747, https://doi.org/10.1175/2008jcli2544.1, 2009.

Yadav, R. K. and Roxy, M. K.: On the relationship between north India summer monsoon rainfall and east equatorial Indian Ocean warming, Global and Planetary Change, 179, 23–32, https://doi.org/10.1016/j.gloplacha.2019.05.001, 2019.

Zhang, Y., Zhang, Y., Feng, M., Feng, M., Du, Y., Phillips, H. E., Phillips, H. E., Bindoff, N. L., and McPhaden, M. J.: Strengthened Indonesian Throughflow Drives Decadal Warming in the Southern Indian Ocean, Geophysical Research Letters, 45, 6167–6175, https://doi.org/10.1029/2018GL078265, 2018.